

## Phonons in $\text{Ge}_{1-x}\text{Si}_x$ bulk crystals

M. Franz, K. F. Dombrowski, H. Rucker, B. Dietrich, and K. Pressel

*Institute for Semiconductor Physics, Walter-Korsing-Strasse 2, 15230 Frankfurt (Oder), Germany*

A. Barz, U. Kerat, P. Dold, and K. W. Benz

*Kristallographisches Institut, Universität Freiburg, Hebelstrasse 25, 79104 Freiburg, Germany*

(Received 13 May 1998; revised manuscript received 5 October 1998)

We compare infrared absorption and Raman spectra of high-quality  $\text{Ge}_{1-x}\text{Si}_x$  bulk crystals ( $0 < x < 0.4$ ). We use this comparison together with lattice-dynamical calculations to report on the behavior of the Ge-Ge phonon at  $300\text{ cm}^{-1}$ , to identify Ge-Si and Si-Si modes, and to clarify contradictory assignments of certain Ge-Si and Si-Si modes. The Ge-Ge optical phonon observed in Raman spectra at  $300\text{ cm}^{-1}$  shifts continuously to lower energies with increasing Si content, also for  $x < 0.03$ . This is in good agreement with theoretical calculations, but in contradiction to previously reported experimental data. The Si local-vibrational mode at about  $390\text{ cm}^{-1}$  is infrared and Raman active. We resolve the local-vibrational modes of the three Si isotopes. Two solely Raman-active phonon modes at about  $400$  and  $455\text{ cm}^{-1}$  are unambiguously identified as modes caused by Si-Si pairs. We are able to resolve the two corresponding infrared active modes of this Si-Si pair at  $310$  and  $370\text{ cm}^{-1}$ . In the range of about  $460\text{ cm}^{-1}$ , we can distinguish further modes caused by three and four Si nearest-neighbor atoms in infrared and Raman experiments. Absorption lines at  $675$ ,  $780$ , and  $845\text{ cm}^{-1}$ , not reported hitherto, are identified as combination modes of phonons with the Si local-vibrational mode. [S0163-1829(99)01816-0]

### I. INTRODUCTION

Si and Ge are miscible over the whole composition range, and they have the same crystal structure and valency. No new electronic states are introduced by alloying Si and Ge. Therefore,  $\text{Ge}_{1-x}\text{Si}_x$  is a prototype material to study the effects of disorder on the vibrational spectrum. In  $\text{Ge}_{1-x}\text{Si}_x$  crystals, Ge-Ge, Ge-Si, and Si-Si vibrational modes are present. The appearance and the properties of these vibrations are strongly influenced by alloy composition.

Several papers have been published investigating the lattice dynamics of bulk  $\text{Ge}_{1-x}\text{Si}_x$  crystals by infrared (IR) absorption,<sup>1-4</sup> Raman,<sup>5-9</sup> and theory.<sup>10,11</sup> Despite these previous investigations, phonon spectra of  $\text{Ge}_{1-x}\text{Si}_x$  crystals still show several discrepancies. We used IR absorption and Raman measurements on the same samples to clarify these discrepancies. We used the anharmonic Keating model<sup>12</sup> to compare IR absorption and Raman measurements with theory. Thus, we were able to identify the origin of different IR and Raman-active Ge-Si and Si-Si vibrations. Furthermore, we can resolve several new peaks in our high-quality samples, which we explain using the anharmonic Keating model.

It is well known that the Raman active Ge optical phonon at  $300\text{ cm}^{-1}$  shifts to lower energies with increasing Si content for  $x > 0.05$  due to disorder in the alloy.<sup>6,7</sup> However, Fuchs *et al.* have reported a shift to higher energies for  $0 \leq x \leq 0.03$ .<sup>9</sup> This result cannot be confirmed by our measurements. We observe a continuous, approximately linear decrease of the Ge optical-phonon energy, even for low Si content  $x < 0.03$ .

Ge-Si vibrations in the alloy have been previously investigated by IR absorption<sup>2-4</sup> and Raman<sup>5-8</sup> measurements.

Gaisler *et al.* observed in their Raman investigations on Ge-rich samples two different Ge-Si vibrational modes at  $390$  and  $400\text{ cm}^{-1}$ .<sup>8</sup> We compare IR absorption and Raman measurements in the spectral range of Ge-Si vibrations. The Ge-Si vibration at  $390\text{ cm}^{-1}$  is IR and Raman active. In accordance to the literature we attribute it to the Si local-vibrational mode (LVM). The second Ge-Si phonon at  $400\text{ cm}^{-1}$  is only Raman active. Based on the observed selection rules and theoretical calculations, we attribute the Ge-Si phonon at  $400\text{ cm}^{-1}$  to nearest-neighbor pairs of Si atoms. This attribution is in agreement with the theoretical study of Grein and Cardona,<sup>11</sup> but in contradiction to the interpretation of Gaisler *et al.*<sup>8</sup> They interpreted the  $400\text{ cm}^{-1}$  mode with the increasing influence of Si atoms in the vicinity of a single Si atom on the Ge-Si bond length, and thus on the energy of the LVM. Furthermore, we detect the two IR-active modes of a Si nearest-neighbor pair in our absorption spectra.

Si-Si vibrations have been reported previously at about  $460\text{ cm}^{-1}$  in Raman measurements.<sup>5-8</sup> These investigations were performed for  $x > 0.05$  and  $T = 300\text{ K}$ . Only broad lines were observed. We clearly resolve an increasing number of Si-Si modes in Raman spectra recorded at  $T = 80\text{ K}$  for  $x \geq 0.03$  with increasing Si content. We are able to assign these Si-Si modes to Si nearest-neighbor pairs, three neighboring Si atoms, etc., by comparing experimental spectra with the theoretical results. Cosand and Spitzer have reported weak absorption lines in the spectral range of Si-Si vibrations at  $460\text{ cm}^{-1}$  in IR absorption spectra for  $x = 0.12$ .<sup>2</sup> But they could not assign these lines due to the weak absorption strength. We clearly resolve the Si-Si lines in IR absorption for samples with Si content  $x > 0.10$  and were able to compare them with the Raman-active Si-Si vibrations.

The dominating phonon-absorption mechanism in Ge is two-phonon absorption. The prominent two-phonon absorp-

tion features in Ge are still present in  $\text{Ge}_{1-x}\text{Si}_x$  for low Si content. An absorption line at  $505 \text{ cm}^{-1}$  has been reported for  $x < 0.01$  and has tentatively been assigned to a two-phonon process with simultaneous absorption of a quasi-LVM and a Si-LVM.<sup>4</sup> With our measurements we are able to manifest this assignment. Furthermore, we observe additional SiGe-specific combination modes at  $675$ ,  $780$ , and  $845 \text{ cm}^{-1}$ , not reported hitherto.

This paper is organized as follows. In Sec. II we describe the experimental details. In Sec. III we briefly summarize the theory of the anharmonic Keating model. The experimental results are described in Sec. IV. We present the results in the order of the wave number of the observed lattice vibrations, beginning with the lowest wave number. The discussion in Sec. V is organized in the same way. Finally, we summarize the results.

## II. EXPERIMENT

The Ge-rich  $\text{Ge}_{1-x}\text{Si}_x$  single crystals with  $x \leq 0.1$  were grown by the vertical Bridgman method in a monoellipsoid mirror furnace.<sup>13</sup> The single crystals with higher Si content  $x > 0.1$  were grown with the zone-leveling method in a double-ellipsoid mirror furnace.<sup>14</sup> The crystals have a diameter of 9 mm. The orientation of the samples is (111). We cut samples with a thickness between 0.7 and 1.2 mm from the crystals. The free-carrier concentration of the samples is less than  $1 \times 10^{15} \text{ cm}^{-3}$  at  $T = 300 \text{ K}$ . Thus, the contribution of electronic transitions to the IR absorption spectra is negligible and only lattice absorption can be studied.

The accurate knowledge of the alloy composition is important for the interpretation of the spectra. We determined the lattice constant for the  $\text{Ge}_{1-x}\text{Si}_x$  samples with  $x \leq 0.1$  by the x-ray diffraction method after Bond.<sup>15</sup> The alloy composition was obtained from the variation of the lattice constant with Si content determined by Dismukes, Ekstrom, and Paff.<sup>16</sup> Additionally, we determined the alloy composition from photoluminescence (PL) measurements as described by Alonso and Weber.<sup>17</sup> The Si content of the samples with  $x > 0.1$  was determined by PL and energy dispersive x-ray analysis EDAX. Measurements of the alloy composition at different spots on the sample surface revealed a high homogeneity in alloy composition. The variation of the Si content  $x$  was  $\Delta x < 0.0015$ .

The IR absorption measurements were performed with a BOMEM DA8.02 Fourier-transform-infrared spectrometer. A liquid-helium cooled Si-Bolometer and a broadband far IR beam splitter were used for the measurements. The Raman spectra were recorded using a Dilor triple-Raman spectrometer with microscope entrance in backscattering configuration. The scattering was excited by the  $514.5\text{-nm}$  line of an  $\text{Ar}^+$  ion laser.

## III. THE ANHARMONIC KEATING MODEL

In this section we briefly summarize the basic features of the used lattice-dynamical model. An anharmonic variant<sup>12</sup> of the Keating model<sup>18</sup> was applied for calculating phonon spectra. The theory of the anharmonic Keating model is described in detail in Ref. 12. It has been demonstrated in Ref. 12 that the effects of strain and alloying of optical phonons

in SiGe are adequately described by this simple two-force-constant model.

The Keating model<sup>18</sup> describes the strain energy of a diamond structure

$$W = \sum_{i,j} \frac{\alpha}{a_0^2} [\Delta(r_{ij}^2)]^2 + \sum_{i,j,k \neq j} \frac{\beta}{a_0^2} [\Delta(\mathbf{r}_{ij} \cdot \mathbf{r}_{ik})]^2 \quad (1)$$

by a bond-stretching force constant  $\alpha$  and a bond-bending force constant  $\beta$ . The vectors  $\mathbf{r}_{ij}$  connect nearest-neighbor lattice sites  $i$  and  $j$ , and  $\Delta$  denotes the change relative to the perfect diamond lattice due to a distortion, i.e.,  $\Delta(\mathbf{r}_{ij} \cdot \mathbf{r}_{ik}) = \mathbf{r}_{ij} \cdot \mathbf{r}_{ik} - \mathbf{r}_{ij}^0 \cdot \mathbf{r}_{ik}^0$  is the change of the scalar product between the two vectors connecting atom  $i$  with its nearest-neighbors  $j$  and  $k$ . In Eq. (1), the sums run over all bonds and  $a_0$  is the equilibrium lattice constant. For an alloy, the force constants  $\alpha$  and  $\beta$  depend on the atomic species forming the corresponding bonds.

The standard Keating model is inadequate for GeSi alloys because of large local distortions due to the different atomic sizes of Si and Ge. As a consequence, the strain energy is not a quadratic form in the deformations. Anharmonic terms must be included for a reasonable description of the lattice dynamic. In the present model, anharmonic effects are included by scaling the force constants  $\alpha$  and  $\beta$  regarding the bond length. From *ab initio* density-functional calculations the scaling laws

$$\alpha_{ij} = \alpha_{ij}^0 \left( \frac{r_{ij}^0}{r_{ij}} \right)^4 \quad \text{and} \quad \beta_{ijk} = \beta_{ijk}^0 \left( \frac{r_{ij}^0}{r_{ij}} \right)^{7/2} \left( \frac{r_{ik}^0}{r_{ik}} \right)^{7/2} \left( \frac{\theta_0}{\theta} \right)^\nu \quad (2)$$

have been derived.<sup>12</sup> The scaling exponents for the bond length dependence of the force constants  $\alpha$  and  $\beta$  have been found to be universal for all alloys of the group IV elements.<sup>12</sup> The exponent  $\nu$  describes the dependence of the bond-bending force constant  $\beta$  on the angle  $\theta$  between two bonds as obtained from a fit to phonon-deformation potentials. In the present paper, we apply the parameters given in Ref. 12.

To simulate the random alloy, we use a 512 atom supercell with randomly distributed atoms according to the stoichiometry. Assuming the same polarizability for all atoms, the off-resonance Raman intensity is given, up to a multiplicative constant, by

$$\sigma^{\alpha\beta\gamma} \sum_{\mu} \frac{2\Gamma\omega}{(\omega_{\mu}^2 - \omega^2)^2 + \Gamma^2\omega^2} \left| \sum_i s_i u_{i\gamma}^{\mu} \right|^2, \quad (3)$$

where  $\mu$  runs over all phonon modes,  $u_{i\gamma}^{\mu}$  is the displacement vector of the atom at lattice site  $i$ , and  $s_i$  is  $+1$  and  $-1$  for the two fcc sublattices of the diamond structure. The Cartesian indices  $\alpha$ ,  $\beta$ , and  $\gamma$  specify the polarization. A Lorentzian lineshape with a broadening  $\Gamma = 3 \text{ cm}^{-1}$  is assumed.

The absorption coefficient for infrared light is given by the imaginary part  $\varepsilon_2$  of the dielectric function. Due to a small polar contribution to the Si-Ge bonds single-phonon absorption becomes possible in GeSi alloys. Describing the charge transfer between Si and Ge by the dynamical charge  $z^*$  and applying Lorentzian broadening,  $\varepsilon_2$  can be expressed as follows:

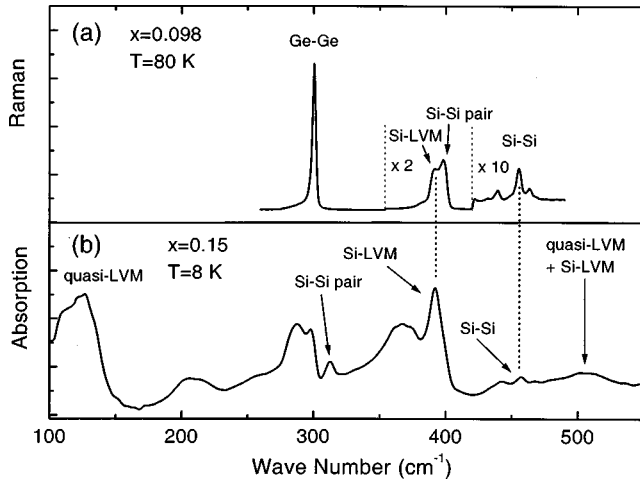


FIG. 1. (a) Overview Raman spectrum of a sample with Si content  $x=0.098$ . Ge-Ge, Ge-Si, and Si-Si vibrations can be distinguished. (b) IR absorption spectrum of a sample with  $x=0.15$ .  $\text{Ge}_{1-x}\text{Si}_x$  specific absorption lines are indicated.

$$\varepsilon_2^{\alpha\beta} \propto \sum_{\mu} \frac{2\Gamma\omega}{(\omega_{\mu}^2 - \omega^2)^2 + \Gamma^2\omega^2} \sum_{i,j} z_i^* z_j^* u_{i\alpha}^{\mu} u_{j\beta}^{\mu}. \quad (4)$$

While this model accounts for the single-phonon absorption due to Si-Ge vibrations it does not describe the two-phonon background of the pure Ge lattice.

#### IV. RESULTS

Figure 1(a) shows a Raman spectrum of a sample with Si content  $x=0.098$ . This spectrum gives an overview of vibrational modes in  $\text{Ge}_{1-x}\text{Si}_x$ : The Ge-Ge vibration at  $300 \text{ cm}^{-1}$  and GeSi specific vibrations at about  $400 \text{ cm}^{-1}$  and  $460 \text{ cm}^{-1}$ . In Fig. 1(b) an IR absorption spectrum of a sample with  $x=0.15$  is depicted. The  $\text{Ge}_{1-x}\text{Si}_x$  specific absorption lines are indicated. Lines, which are absent in pure Ge, appear at about  $115, 310, 390, 460,$  and  $505 \text{ cm}^{-1}$ . The development of room-temperature IR absorption spectra in the range  $100\text{--}600 \text{ cm}^{-1}$  as a function of Si content is depicted in Fig. 2. The IR absorption of Ge in this spectral range is determined by two-phonon absorption due to the lack of a linear electric moment in the crystal with diamond symmetry. The two-phonon absorption features of Ge are still present in  $\text{Ge}_{1-x}\text{Si}_x$  samples with low-Si content, but the sharp peaks associated with the maxima of the combined density of phonons smear out in the alloy.

Two-phonon absorption decreases with decreasing temperature, whereas single-phonon absorption as a first-order process is temperature independent. In Fig. 3 the temperature dependence of the lattice absorption is shown for a sample with Si content  $x=0.15$  in the temperature range between  $T=300$  and  $8 \text{ K}$ . The overall lattice absorption decreases with decreasing temperature. Due to the incorporation of Si in the Ge lattice, the symmetry of  $\text{Ge}_{1-x}\text{Si}_x$  crystals is lowered. As a consequence, temperature-independent single-phonon absorption is observable at  $115, 390,$  and  $460 \text{ cm}^{-1}$ . As shown in Fig. 3, these  $\text{Ge}_{1-x}\text{Si}_x$  specific absorption lines vary less strongly with temperature than the rest of the spectrum. The decrease of the absorption strength of these lines between  $T=300$  and  $120 \text{ K}$  is mainly due to the reduction of

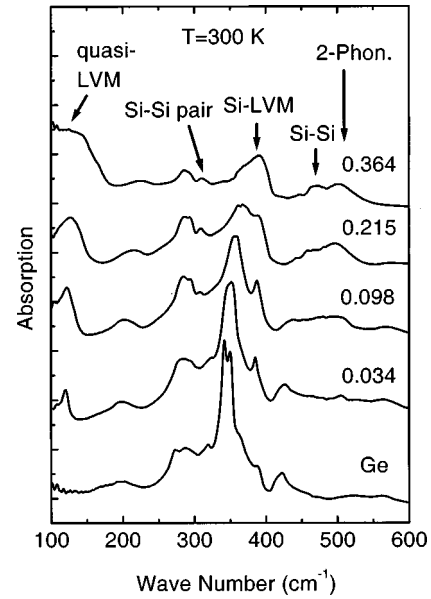


FIG. 2. Absorption spectrum of Ge and spectra of  $\text{Ge}_{1-x}\text{Si}_x$  samples with different alloy composition recorded at  $T=300 \text{ K}$ . The Si content  $x$  of the samples is given at the spectra. The spectra are shifted upwards for better overall view. Arrows indicate the position of the lines discussed in the text.

the overall two-phonon absorption background in the shown spectral range.

The absorption line at  $115 \text{ cm}^{-1}$  is already present for low-Si content of  $x=0.005$ . The strength of this absorption increases and the line broadens strongly with increasing Si content (Fig. 2). This absorption line and its temperature dependence was first detected and investigated by Shen and Cardona<sup>3</sup> for two samples with Si content  $x=0.11$  and  $0.16$ . They attributed this absorption to a quasi-LVM associated with the TA band.

The incorporation of Si in Ge gives rise to Ge-Si and Si-Si vibrations, but also the properties of Ge-Ge vibrations are affected by the Si atoms. The most intense line in Raman spectra of Ge-rich samples at  $300 \text{ cm}^{-1}$  is caused by the Ge optical phonon at the center of the Brillouin zone. The influ-

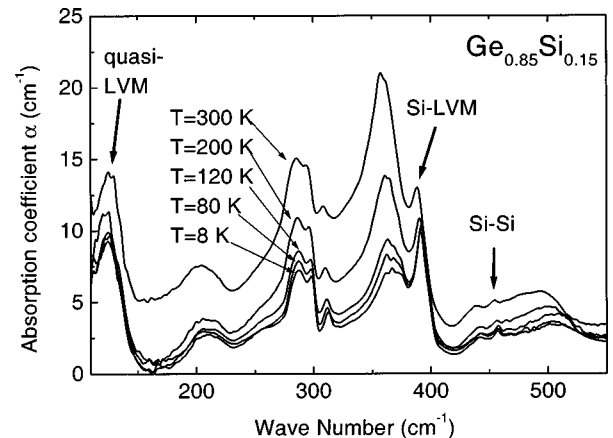


FIG. 3. Absorption spectra for a  $\text{Ge}_{1-x}\text{Si}_x$  sample with  $x=0.15$  at different temperatures. Temperature-independent single-phonon absorption (arrows) and temperature-dependent two-phonon absorption is observable in  $\text{Ge}_{1-x}\text{Si}_x$ .

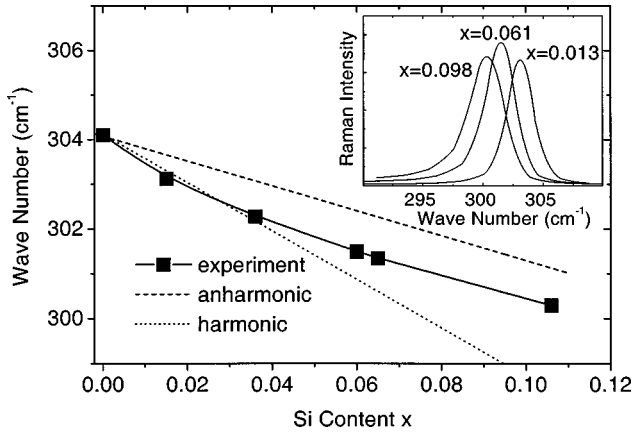


FIG. 4. The Ge phonon shifts continuously to lower energies with increasing Si content. Peak positions of measured Raman spectra (symbols) are shown together with results of calculations with anharmonic Keating model (dashed line) and calculations with zero anharmonicity (dotted line). Inset: Raman spectra of the Ge-Ge phonon for different alloy composition recorded at  $T=80$  K.

ence of alloy composition on the energy of this Ge phonon is shown in Fig. 4. The energy decreases continuously with increasing Si content, and also for small Si contents of  $x < 0.03$ .

A significant difference between the lattice absorption of Ge and  $\text{Ge}_{1-x}\text{Si}_x$  is the appearance of a line at about  $390 \text{ cm}^{-1}$ , which is the LVM of an isolated Si atom in the Ge lattice.<sup>2</sup> This absorption line shifts slightly to higher energies and broadens strongly with increasing Si content (Fig. 2). The Si-LVM absorption is a first-order process and, thus temperature independent. This is observed in the temperature-dependent absorption spectra of Fig. 3. The Si-LVM turns into a Ge-Si-like phonon, which is observable over a wide composition range. Cosand and Spitzer reported an absorption line near  $400 \text{ cm}^{-1}$  for Si-rich crystals.<sup>2</sup> The Si-LVM is also Raman active.<sup>5,7</sup> A Raman spectrum of the Si-LVM recorded at 80 K for a sample with Si content  $x=0.013$  is presented in Fig. 5. Next to the intensive line at  $387.3 \text{ cm}^{-1}$ , the spectrum exhibits two satellite peaks at lower energy. These three lines are the LVM's of the natural Si isotopes  $^{28}\text{Si}$ ,  $^{29}\text{Si}$ , and  $^{30}\text{Si}$  with the abundances of 92.2%, 4.7%, and 3.1%, respectively. The intensity ratios of the three lines in Fig. 5 correspond to the abundances of the isotopes and the energy shift agrees with the different masses of the isotopes, i.e.,  $\omega_{29}/\omega_{28} = \sqrt{m_{28}/m_{29}}$  and  $\omega_{30}/\omega_{28} = \sqrt{m_{28}/m_{30}}$ . This observation of the isotope effect is reported for the first time and demonstrates the excellent quality of the crystals, since the effect is not observable in crystals of poor quality due to line broadening.

In Figs. 6(a) and 6(b) is a comparison between the IR and Raman-active modes in the spectral range between  $360$  and  $420 \text{ cm}^{-1}$ . The Si-LVM at  $390 \text{ cm}^{-1}$  is present in absorption and Raman spectra. In the absorption spectra an additional weak line is observable at  $370 \text{ cm}^{-1}$ . In the Raman spectra, a second line appears at  $400 \text{ cm}^{-1}$ , which increases strongly in intensity with increasing Si content. This vibration is only Raman but not IR active.

Figure 7 shows Raman spectra at  $T=80$  K and IR absorption spectra at  $T=10$  K in the spectral range of Si-Si vibra-

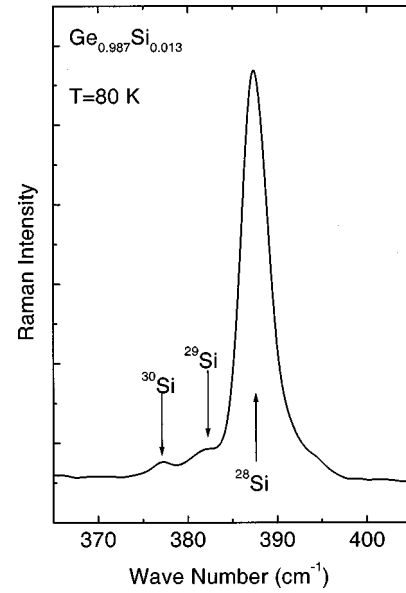


FIG. 5. Raman spectrum of a  $\text{Ge}_{1-x}\text{Si}_x$  sample with  $x=0.013$  recorded at 80 K. The Si local vibrational mode (LVM) is shown. Next to the LVM of the  $^{28}\text{Si}$  isotope with natural abundance of 92.2%, the LVM's of the isotopes  $^{29}\text{Si}$  (4.7%) and  $^{30}\text{Si}$  (3.1%) are observable.

tions. A line at  $455 \text{ cm}^{-1}$  appears in the Raman spectrum of a sample with Si content of  $x=0.034$  recorded at  $T=80$  K. The intensity of this line increases with increasing Si content and more lines appear in the spectra. These lines are also observable in IR absorption as demonstrated in the low-temperature absorption spectra of Fig. 7, but are only detectable for Si content  $x > 0.1$  due to the weak absorption strength and the two-phonon background.

Another  $\text{Ge}_{1-x}\text{Si}_x$  specific absorption exists at  $505 \text{ cm}^{-1}$  (Fig. 8). This absorption mode has previously been reported by Humlicek *et al.*<sup>4</sup> They tentatively attributed the absorption at  $505 \text{ cm}^{-1}$  to a combination mode of the quasi-LVM and the Si-LVM. In Fig. 8, these lines are shown for a sample with low Si content of  $x=0.005$ . For this Si content, the quasi-LVM and the Si-LVM are also present in the spec-

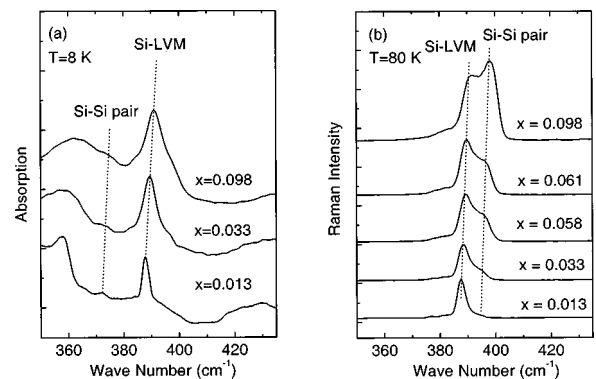


FIG. 6. (a) Absorption spectra at  $T=8$  K and (b) Raman spectra at  $T=80$  K of  $\text{Ge}_{1-x}\text{Si}_x$  samples with different Si content  $x$ . The Si-LVM is infrared and Raman active. A second, only Raman-active vibration appears with increasing Si content. The IR-active mode at  $370 \text{ cm}^{-1}$  and the Raman-active mode at  $400 \text{ cm}^{-1}$  are caused by Si nearest-neighbor pairs.

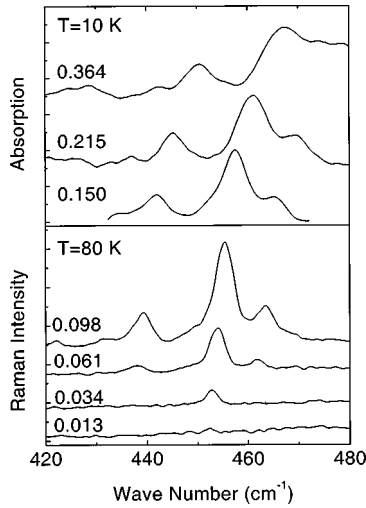


FIG. 7. Raman spectra at  $T=80$  K and IR absorption spectra at  $T=10$  K for  $\text{Ge}_{1-x}\text{Si}_x$  samples with different alloy composition in the wave-number range of Si-Si vibrations. The two-phonon background is subtracted for the absorption spectra. The different modes are caused by an increasing number of neighboring Si atoms.

trum. The energetic position of the absorption line at  $505 \text{ cm}^{-1}$  corresponds to the sum of the energy of the quasi-LVM and the Si-LVM for  $x < 0.06$  (inset Fig. 8).

In the wave-number regime higher than  $600 \text{ cm}^{-1}$ , four SiGe specific lines are observable, which are, to the best of our knowledge, reported for the first time (Fig. 9). These lines appear with increasing Si content at  $675$ ,  $780$ ,  $825$ , and  $845 \text{ cm}^{-1}$ .

## V. DISCUSSION

### A. Ge optical phonon at $300 \text{ cm}^{-1}$

Raman spectra of Ge-rich samples are dominated by the mode at  $300 \text{ cm}^{-1}$ , due to the zone-center optical phonon in Ge. Two effects influence the energy of the Ge phonon in the alloy:<sup>19</sup> (a) One effect is the reduction of the lattice constant due to the incorporation of Si atoms in the Ge lattice. The

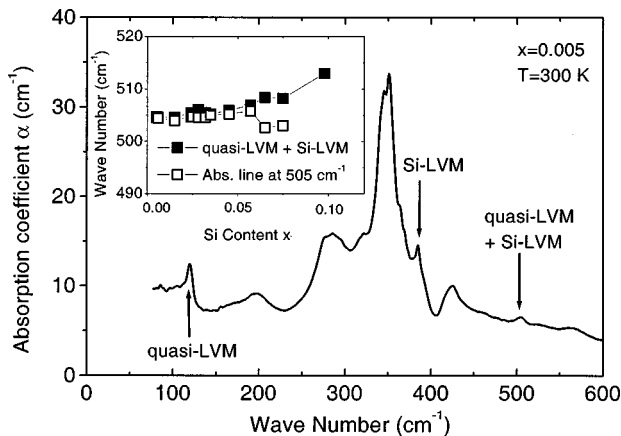


FIG. 8. Absorption spectrum at  $T=300$  K for a  $\text{Ge}_{1-x}\text{Si}_x$  sample with low-Si content of  $x=0.005$ . The inset shows the wave-number sum of the quasi-LVM and the Si-LVM (■) and the position of the line at about  $505 \text{ cm}^{-1}$  (□) as a function of the Si content  $x$ .

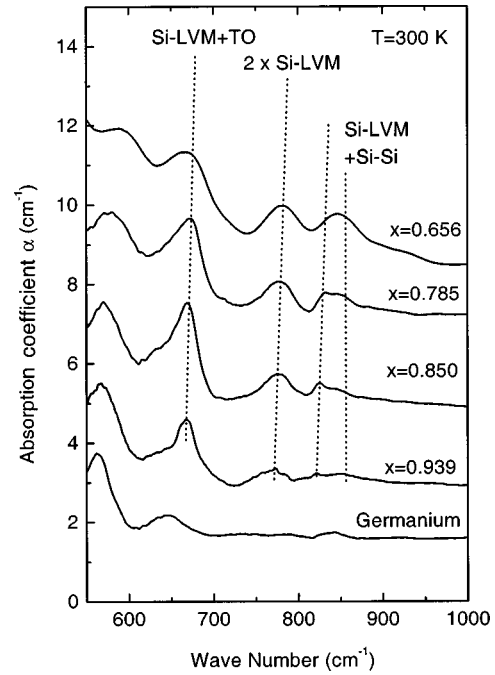


FIG. 9. Absorption spectra in the wave-number range of combination modes. GeSi-specific lines appear at  $675$ ,  $780$ ,  $825$ , and  $845 \text{ cm}^{-1}$ . With the exception of the line at  $825 \text{ cm}^{-1}$ , the energy of these absorptions correspond to combination modes as indicated in the figure.

average bond length decreases, which results in an increase of the bond stiffness. Thus, the reduction of the lattice constant leads to an increase of the Ge phonon energy with increasing Si content. (b) The second effect is disorder in the alloy due to random distribution of Si and Ge atoms on the lattice sites. The Ge-Ge vibrations are confined to the subspace of the Ge-Ge bonds. This effect lowers the Ge-phonon energy.<sup>19</sup>

As shown in Fig. 4, the phonon energy of the Ge-Ge mode at  $300 \text{ cm}^{-1}$  decreases continuously with increasing Si content. This demonstrates that the disorder effect overrides the increase of the bond stiffness due to the reduction of the lattice constant, even for low Si content of  $x < 0.03$ . This continuous decrease was previously observed for Si content  $x > 0.05$  by different groups.<sup>6,7</sup> However, Fuchs *et al.* observed an increase of the Ge phonon energy for bulk  $\text{Ge}_{1-x}\text{Si}_x$  crystals from  $x=0$  to  $0.03$ .<sup>9</sup> Only for  $x > 0.03$  they observed a decrease of the energy. The spectra of Fuchs *et al.*<sup>9</sup> were recorded at  $T=80$  K as our spectra in Fig. 4. Fuchs *et al.* observed an asymmetry of the Raman line on the high-energy side for their samples with  $x < 0.03$ .<sup>9</sup> This asymmetry on the high-energy side is not observed in our spectra. Due to disorder in the alloy, the momentum conservation for the Raman process is relaxed. Phonons with nonvanishing momentum contribute to the Raman signal, which causes an asymmetry on the low-energy side of the Raman line as observed for our samples. Our experimental results indicate that reduction of the phonon energy due to disorder is the dominating effect on Ge-Ge vibrations in our samples, and also for low-Si content.

The experimentally determined shift of the Ge phonon is compared with results of calculations in Fig. 4. One set of calculations was done with the anharmonic Keating model.

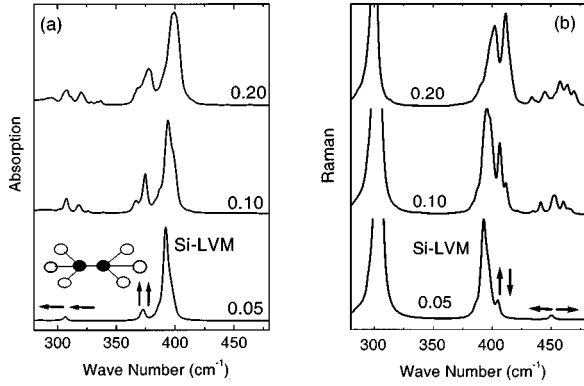


FIG. 10. (a) Absorption and (b) Raman spectra calculated with the anharmonic Keating model for different alloy compositions. The IR or Raman-active vibrational modes of a Si-nearest-neighbor pair are indicated by arrows at the corresponding lines.

Details of the calculations were described in Ref. 12. Supercells of 512 atoms were used. Raman spectra were obtained by averaging over ten supercells with randomly distributed atoms. To clarify the role of the anharmonicity we have also performed calculations with a harmonic model and identical force constants. The anharmonicity was turned off by setting the exponents in Eq. (2) to zero. Both calculations result in a continuous decrease of the Ge phonon energy. This result is qualitatively different to earlier calculations by Fuchs *et al.*,<sup>9</sup> though both calculations used a Keating model and supercells. We are not able to resolve this discrepancy. We have tested the sensitivity of our calculations to the numerical values of the two force constants  $\alpha$  and  $\beta$ . A monotonously decreasing frequency of the Ge-Ge mode with increasing Si content was found for all ratios  $\alpha/\beta$  between 2 and 12.

### B. Ge-Si vibrations at 390 and 400 $\text{cm}^{-1}$

Different Ge-Si vibrations exist in the alloy. The IR and Raman-active Si-LVM at 390  $\text{cm}^{-1}$  and a second, only Raman-active Ge-Si phonon at 400  $\text{cm}^{-1}$  (Fig. 6). Gaisler *et al.* observed the two Raman-active modes at 390 and 400  $\text{cm}^{-1}$  in Raman spectra recorded at 80 K.<sup>8</sup> They interpreted this effect with the increasing influence of Si atoms in the vicinity of a single Si atom on the Ge-Si bond length, and thus on the energy of the Si-LVM. But following this interpretation the high-energy lines should be observable in absorption measurements.

The different IR and Raman-active Ge-Si vibrations can theoretically be described with the anharmonic Keating model. Figure 10 shows calculated IR absorption and Raman spectra for different alloy compositions. These calculated spectra agree well with the experimental results. The calculated spectra reveal the Si-LVM at 390  $\text{cm}^{-1}$  for absorption and Raman. Next to isolated Si atoms, vibrations of Si pairs on second-nearest-neighbor (2 nn) sites, 3 nn sites, etc., contribute to the 390  $\text{cm}^{-1}$  line. The vibration of a 2 nn Si pair is slightly shifted to higher energy compared with the Si-LVM. The mode energy is almost unchanged if there is more than one Ge atom between two Si atoms. Next to the Si-LVM, additional lines are present in the calculated IR absorption spectra at about 310 and 370  $\text{cm}^{-1}$  and in the Raman spectra at 400 and 460  $\text{cm}^{-1}$ . These lines are caused by

Si nn-pair vibrations. This assignment is in agreement with a previous publication of Grein and Cardona, who used a Green's function approach to calculate the vibrations of different Si clusters.<sup>11</sup>

A Si nn pair in the Ge lattice has  $D_{3d}$  symmetry. Thus, two IR-active and two Raman-active vibrations exist for this defect.<sup>20</sup> These vibrational modes are indicated by the arrows in the calculated spectra of Fig. 10. We are able to detect the IR active modes of the Si nn pair in our absorption spectra. In Figs. 1(b) and 2 an absorption line is observable at 308  $\text{cm}^{-1}$  and weak absorption is present at 370  $\text{cm}^{-1}$  in the absorption spectra of Fig. 6(a). In the calculated and experimental Raman spectra, the line at 400  $\text{cm}^{-1}$  increases strongly in intensity with increasing Si content and lines at about 460  $\text{cm}^{-1}$  appear.

A Ge-Si vibration is also observable in PL spectra. The phonon coupling to excitonic emission in low-temperature PL spectra reveals the phonons of Ge-Ge, Ge-Si, and Si-Si vibrations. Weber and Alonso determined the energy of the Ge-Si phonon observed in PL for  $0.05 < x < 0.75$ .<sup>17</sup> They compared their results with the Raman energies of the Ge-Si vibrations reported by other groups and found different energies for the PL and Raman Ge-Si vibrations. We directly compared the Ge-Si phonon observed in PL, IR absorption, and Raman for our Ge-rich samples. Although the PL linewidth is about a factor of 3.5 larger than the IR and Raman lines, the maximum of the PL line agrees with the IR and Raman-active Ge-Si vibration at about 390  $\text{cm}^{-1}$ .

### C. Si-Si vibration at 460 $\text{cm}^{-1}$

Raman and IR absorption spectra reveal several lines in the wave number range of 460  $\text{cm}^{-1}$  (Fig. 7). Different groups previously observed Raman-active modes in this spectral range at  $T = 300$  K.<sup>5-8</sup> These modes were first reported by Feldman, Ashkin, and Parker, who observed a band at 462  $\text{cm}^{-1}$  for  $x \geq 0.05$ , which consists of two unresolved lines.<sup>5</sup> They tentatively attributed these lines to different Raman-active modes of Si nearest-neighbor-pair vibrations. Further investigations were performed on samples with Si content  $x > 0.1$ . The observed broad bands were attributed to vibrations of Si-Si bonds.<sup>6-8</sup> We clearly resolve an increasing number of modes in the spectral range of 460  $\text{cm}^{-1}$  for  $x \geq 0.03$  in our Raman spectra at  $T = 80$  K (Fig. 7). The most intensive lines are at 439, 455, and 464  $\text{cm}^{-1}$  for  $x = 0.098$ . They shift slightly to higher energies with increasing Si content. The calculated Raman spectra obtained with the anharmonic Keating model in Fig. 10(b) reveal these Raman modes. The calculated spectra show a single line for  $x = 0.05$ . With increasing Si content, the intensity of these lines increases and more modes appear at the high- and low-energy side of the initial line. From the evaluation of the calculated eigenfrequencies and eigenvectors we identify the line at 455  $\text{cm}^{-1}$  as the Si nearest-neighbor pair vibration. The lines at 439 and 464  $\text{cm}^{-1}$  are two different modes originating from three neighboring Si atoms. For higher Si content of  $x \geq 0.23$ , a detailed experimental and theoretical study of Raman spectra in the wave-number range of Si-Si vibrations has been done by Alonso and Winer.<sup>7</sup> Further theoretical investigations have been done by Grein and Cardona.<sup>11</sup>

Cosand and Spitzer observed weak absorption bands at about  $450\text{ cm}^{-1}$  for  $x=0.12$ ,<sup>2</sup> but they could not attribute these lines due to the weak absorption strength. In our low-temperature IR spectra of Fig. 7, the same Si-Si vibrations are observable as in Raman spectra. The two-phonon background is subtracted in the absorption spectra. The Si-Si modes are only observable for  $x>0.1$  in IR absorption due to the two-phonon background and the weak absorption strength. The vibrational mode of a Si nearest-neighbor pair as indicated in Fig. 10(b) for the peak at  $460\text{ cm}^{-1}$  is the origin of the observed Raman-active line at  $455\text{ cm}^{-1}$  for low-Si content. This vibration is not IR active due to the  $D_{3d}$  symmetry of an isolated Si pair in Ge. With increasing Si not only do modes of isolated Si nearest-neighbor pairs contribute to the line at  $455\text{ cm}^{-1}$ , but also Si-Si vibrations involving more than two Si atoms occur at this wave number. These Si-Si vibrations can be IR active.

The IR-active Si-Si vibrations shift to higher energies with increasing Si content and the maximum is at  $467\text{ cm}^{-1}$  for  $x=0.364$ . This line probably develops into the absorption at  $485\text{ cm}^{-1}$ , observed by Cosand and Spitzer<sup>2</sup> on the Si-rich side of the alloy composition. They attributed this line to impurity-induced single-phonon absorption. No structure is present in the wave-number range of  $460\text{ cm}^{-1}$  in the calculated IR-absorption spectra [Fig. 10(a)]. This is due to the chosen absorption selection rules (Sec. III). Only Ge-Si displacements contribute to the calculated IR-absorption spectra.

#### D. Combination modes for wave numbers higher than $500\text{ cm}^{-1}$

Humlicek *et al.*, who investigated samples with Si content up to  $x=0.01$ , tentatively attributed the absorption line at  $505\text{ cm}^{-1}$  to the combination mode of the quasi-LVM at  $115\text{ cm}^{-1}$  and the Si-LVM at  $390\text{ cm}^{-1}$ .<sup>4</sup> They recorded their absorption spectra only for wave numbers higher than  $350\text{ cm}^{-1}$ . Thus, Humlicek *et al.* did not observe the quasi-LVM in their spectra, which is desirable to confirm their attribution for the  $505\text{ cm}^{-1}$  absorption. This is demonstrated in Fig. 8. The  $505\text{ cm}^{-1}$  is detectable for low-Si content of  $x=0.005$ . For this low-Si content the quasi-LVM is already present in the spectra. The sum of the energies of the quasi-LVM and the Si-LVM corresponds to the energy of the line at  $505\text{ cm}^{-1}$  up to  $x=0.06$  (inset Fig. 8). For  $x>0.06$  the absorption maximum in the range of  $500\text{ cm}^{-1}$  does not correspond to the sum of the quasi-LVM and the Si-LVM anymore. The overall absorption in the wave-number range of  $500\text{ cm}^{-1}$  increases with rising Si content (Fig. 2). This new developing absorption decreases with decreasing temperature (Fig. 3), indicating a two-phonon process. It can mask the line at  $505\text{ cm}^{-1}$  observed for low-Si content.

The absorption line at  $675\text{ cm}^{-1}$  (Fig. 9) appears already at low-Si content, as the Si-LVM. The energy difference between this line and the Si-LVM is  $285\text{ cm}^{-1}$ . This corresponds to the energy of a singularity in the density of states for the TO phonon. Thus, we attribute the absorption line at  $675\text{ cm}^{-1}$  to the combination of the Si-LVM and TO phonon. Such kind of two-phonon process was previously observed by Waldner, Hiller, and Spitzer in lithium-boron-doped Si.<sup>21</sup> They found lines at the energy sum of lithium-

boron LVM's and Si critical-point phonon frequencies. The  $780\text{ cm}^{-1}$  absorption line corresponds to twice the energy of the Si-LVM of  $390\text{ cm}^{-1}$ . A very weak SiGe specific absorption line appears at  $825\text{ cm}^{-1}$ . With increasing Si content, this line is masked by an absorption line developing at  $845\text{ cm}^{-1}$ . The latter can originate from the combination of the Si-Si vibrations at  $455\text{ cm}^{-1}$  and Si-LVM at  $390\text{ cm}^{-1}$ . The origin of the  $825\text{ cm}^{-1}$  is unknown.

#### V. SUMMARY

The incorporation of Si in Ge influences the Ge-Ge vibrations and gives rise to Ge-Si and Si-Si vibrations. Comparing IR absorption, Raman, and theoretical results, we have investigated in detail these lattice vibrations in Ge-rich single crystals of high quality. The high crystal quality is seen from the observation of the isotope effect of the Si-LVM.

The Ge optical phonon measured by Raman spectroscopy shifts to lower energies with increasing Si content. This shows the dominance of disorder effects in the alloy, even for low-Si content of  $x<0.03$ , which is in good agreement with theoretical calculations, but in contradiction to a previous publication.<sup>9</sup>

We have compared IR absorption and Raman measurements in the spectral range of Ge-Si phonons. The Ge-Si vibration at  $390\text{ cm}^{-1}$ , developing from the LVM of an isolated Si atom is IR and Raman active. A second Ge-Si phonon at  $400\text{ cm}^{-1}$  is only Raman active. We have identified this Raman-active mode using lattice-dynamical calculations. It is caused by at least two Si atoms at nearest-neighbor lattice sites.

Nearest-neighbor Si atoms also cause vibrations at about  $460\text{ cm}^{-1}$ . For Ge-rich samples with low-Si content, we resolve an increasing number of Si-Si modes with increasing Si content in low-temperature Raman measurements in the spectral range of  $460\text{ cm}^{-1}$ . We used an anharmonic Keating model to identify these different modes. The most intense Si-Si line at about  $455\text{ cm}^{-1}$  originates from Si nearest-neighbor-pair vibrations. The other can be attributed to vibrations of increasing number of neighboring Si atoms. The Si nearest-neighbor pair causes, in addition to two Raman-active modes, two IR active modes. We are able to observe these two modes in absorption measurements at  $308\text{ cm}^{-1}$  and as a very weak line at  $370\text{ cm}^{-1}$ .

We confirm the attribution of Humlicek *et al.*<sup>4</sup> for the  $505\text{-cm}^{-1}$  absorption as a combination mode by the simultaneous observation of the three lines: the quasi-LVM at  $115\text{ cm}^{-1}$ , the Si-LVM at  $390\text{ cm}^{-1}$ , and the combination mode at  $505\text{ cm}^{-1}$ . We observe further combination modes at  $675$ ,  $780$ , and  $845\text{ cm}^{-1}$ , which are attributed to the combination of the Si-LVM with a TO phonon, two Si-LVM and the Si-LVM plus Si-Si vibrations, respectively.

#### ACKNOWLEDGMENTS

The authors are indebted to Dr. J. Kräußlich of the University of Jena for the x-ray diffraction measurements and L. Rees-Isele for ampoule preparation. The financial support of the DFG (Grant No. BE 896/7, PR 493/3) and DARA (Grant No. 50 WM 9505) is gratefully acknowledged.

- <sup>1</sup>R. Braunstein, Phys. Rev. **130**, 879 (1963).
- <sup>2</sup>A. E. Cosand and W. G. Spitzer, J. Appl. Phys. **42**, 5241 (1971).
- <sup>3</sup>S. C. Shen and M. Cardona, Solid State Commun. **36**, 327 (1980).
- <sup>4</sup>J. Humlicek, K. Navratil, M. G. Kekoua, and E. V. Khoutsishvili, Solid State Commun. **76**, 243 (1990).
- <sup>5</sup>D. W. Feldman, M. Ashkin, and J. H. Parker, Jr., Phys. Rev. Lett. **17**, 1209 (1966).
- <sup>6</sup>W. J. Brya, Solid State Commun. **12**, 253 (1972).
- <sup>7</sup>M. I. Alonso and K. Winer, Phys. Rev. B **39**, 10 056 (1989).
- <sup>8</sup>V. A. Gaisler, O. A. Kuznetsov, I. G. Neizvestnyl, L. K. Orlov, M. P. Sinyukov, and A. B. Talochin, Fiz. Tverd. Tela. (Leningrad) **31**, 292 (1989) [Sov. Phys. Solid State **31**, 2006 (1989)].
- <sup>9</sup>H. D. Fuchs, C. H. Grein, M. I. Alonso, and M. Cardona, Phys. Rev. B **44**, 13 120 (1991).
- <sup>10</sup>S. de Gironcoli, Phys. Rev. B **46**, 2412 (1992).
- <sup>11</sup>C. H. Grein and M. Cardona, Phys. Rev. B **45**, 8328 (1992).
- <sup>12</sup>H. Rücker and M. Methfessel, Phys. Rev. B **52**, 11 059 (1995).
- <sup>13</sup>P. Dold, A. Barz, S. Recha, K. Pressel, M. Franz, and K. W. Benz, J. Cryst. Growth **192**, 126 (1998).
- <sup>14</sup>A. Barz, U. Kerat, P. Dold, and K. W. Benz, Cryst. Res. Technol. **33**, 849 (1998). (to be published).
- <sup>15</sup>W. L. Bond, Acta Crystallogr. **13**, 814 (1960).
- <sup>16</sup>J. P. Dismukes, L. Ekstrom, and R. I. Paff, J. Phys. Chem. **68**, 3021 (1964).
- <sup>17</sup>J. Weber and M. I. Alonso, Phys. Rev. B **40**, 5683 (1989).
- <sup>18</sup>P. N. Keating, Phys. Rev. **145**, 637 (1966).
- <sup>19</sup>J. Menendez, A. Pinczuk, J. Bevk, and J. P. Mannaerts, J. Vac. Sci. Technol. B **6**, 1306 (1988).
- <sup>20</sup>R. C. Newman, *Infrared Studies of Crystal Defects*, edited by B. R. Cales (Taylor & Francis, London, 1973).
- <sup>21</sup>M. Waldner, M. A. Hiller, and W. G. Spitzer, Phys. Rev. **140**, A172 (1965).